

Collisional excitation of doubly deuterated ammonia ND₂H by para-H₂

L. Wiesenfeld¹, E. Scifoni^{1,2}, A. Faure¹, and E. Roueff³

¹ *Laboratoire d'Astrophysique de Grenoble, CNRS/Université Joseph-Fourier, Grenoble, France.*

² *Department of Biophysics, Gesellschaft für Schwerionenforschung, Darmstadt, Germany.*

³ *LUTH, CNRS/Observatoire de Paris, Meudon, France*

26 March 2022

ABSTRACT

Collisional de-excitation rates of partially deuterated molecules are different from the fully hydrogenated species because of lowering of symmetry. We compute the collisional (de)excitation rates of ND₂H by ground state para-H₂, extending the previous results for Helium. We describe the changes in the potential energy surface of NH₃-H₂ involved by the presence of two deuterium nuclei. Cross sections are calculated within the full close-coupling approach and augmented with coupled-state calculations. Collisional rate coefficients are given between 5 and 35 K, a range of temperatures which is relevant to cold interstellar conditions. We find that the collisional rates of ND₂H by H₂ are about one order of magnitude higher than those obtained with Helium as perturber. These results are essential to radiative transfer modelling and will allow to interpret the millimeter and submillimeter detections of ND₂H with better constraints than previously.

1 INTRODUCTION

Doubly deuterated ammonia has been detected for the first time by Roueff et al. (2000) towards the dark cloud L 134N via its $1_{10} - 1_{01}$ ortho and para transitions at 110 GHz and subsequently in the protostellar environment L1689N by Loinard et al. (2001). The submillimeter fundamental transitions have then been detected at the Caltech Sub-millimeter Observatory by Roueff et al. (2005); Lis et al. (2006) and on the APEX antenna in Chile by Gerin et al. (2006) towards the Barnard 1 molecular cloud and L1689N. ND₂H was shown to be a sensitive tracer of the physical conditions of this star forming region. In a previous paper (Machin & Roueff 2007) some of us have presented the collisional formalism and computed the collisional excitation cross-sections and rate coefficients of ND₂H by He by introducing the appropriate changes in the potential energy surface of NH₃-He, computed by Hodges & Wheatley (2001). This new accurate intermolecular potential energy surface (PES) for NH₃-He has also been used previously to reevaluate the collisional excitation of NH₃ and NH₂D by He (Machin & Roueff 2005; Scifoni et al. 2007; Machin & Roueff 2006). Here, we present results for ND₂H in collision with para-H₂. H₂ is the main constituent of dark clouds environment where ND₂H has been detected. Collisional excitation is dominated by interaction with low temperature H₂; this motivated our present study, aimed particularly at the low temperature excitation schemes of ND₂H.

The paper is organized as follows. In section 2 we briefly describe the changes introduced by the presence of two deuterons in the PES of NH₃-H₂, published recently (Maret et al. 2009). We present in section 3 the collisional equations for the ND₂H-H₂ system. The cross sections and the corresponding reaction rate coefficients of the ND₂H-H₂ system are given in section 4. We present our conclusions in Section 5

2 POTENTIAL ENERGY SURFACE

We have recently put forward a potential energy surface (PES) of NH₃ in interaction with H₂. This rigid rotor PES is reported in full details in Maret et al. (2009). Here we need to transform this PES from the triple H isotopologue of ammonia to the doubly deuterated one, ND₂H. For a given *inter*-molecular geometry, the interaction between the molecules of ammonia and H₂ depends on the various electronic charges (electrons and nuclei) as well as of the *intra*-molecular geometries of ammonia and molecular hydrogen. For the two isotopologues NH₃ and ND₂H the charge structure is identical, as long as we remain in the Born-Oppenheimer approximation. However, the geometries are different in two aspects: (i) the intra-molecular distances change slightly and (ii) the position of the centre of mass of ND₂H is shifted with respect to the centre of mass of NH₃ and the principal axes of inertia are rotated. Let us treat both points in succession.

The original PES for NH₃-H₂ was computed with both monomer geometries taken at their average value in the ground vibrational state (Maret et al. 2009). This has been demonstrated to be a much better approximation than taking equilibrium geometries: in the case of the similar H₂O-H₂ system, Faure et al. (2005); Valiron et al. (2008) have found that employing state-averaged geometries is a very good approximation for including vibrational effects within a rigid rotor PES. We note that the importance of the zero-point vibrational correction was discussed earlier by Meuwly & Bemish (1997), in the N₂H⁺-He system.

In particular the $r(\text{HH})$ distance for molecular hydrogen was shown to provide the largest vibrational correction. It was taken by Maret et al. (2009) at its average value of 1.4488 Bohr. Similarly, the NH₃ molecule was taken at its ground-state average geometry with the following parameter: $r(\text{NH}) = 1.9512$ Bohr,

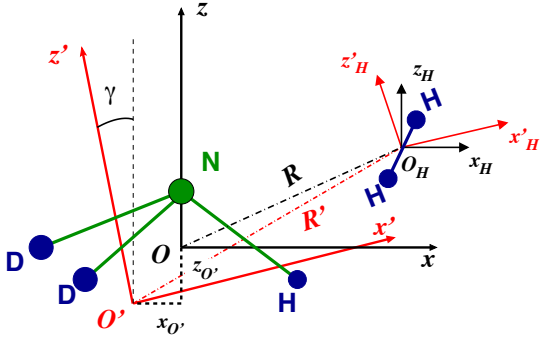


Figure 1. Scheme of the coordinate transformation between the frame $O'x'y'z'$ of ND_2H , and the original frame $Oxyz$, of the $\text{NH}_3\text{-H}_2$ system, see Eqs. (2), (3). Only the Oxz and $O'x'z'$ axes are represented, since the y axes do not change. Distances are not to scale.

$\widehat{\text{HNH}} = 107.38$ deg. For ND_2H , the equilibrium geometry is identical to NH_3 since the equilibrium bond lengths and angles depend only on the electronic structure, within the Born-Oppenheimer approximation. However the anharmonic averaging over the ground state vibrational state changes slightly those values, because of mass effects on the vibrational functions. For $\text{H}_2\text{O}/\text{D}_2\text{O}$, these effects have been shown to be essentially negligible with respect to the shift of the center of mass (Scribano et al. 2010). As a result, the above ground-state averaged geometry of NH_3 can be employed for any isotopologue of ammonia and was adopted here.

The second point deals with the fitting of the *ab initio* points onto a functional suited for the scattering calculations. The PES points resulting from the *ab initio* procedure are described in the following coordinate set: R , the distance between the centre of mass of NH_3 and the centre of mass of H_2 , θ , ϕ , the corresponding spherical angles. For NH_3 , θ is defined with respect to Oz , the C_{3v} axis of symmetry of NH_3 , with the nitrogen atom at positive values of z . The angle ϕ is the polar coordinate in the perpendicular Oxy plane, with one of the hydrogen atoms of NH_3 lying in the Ozx plane. Similarly, the H_2 molecule is oriented by the spherical angles θ_H , ϕ_H , in a reference frame $O_Hx_Hy_Hz_H$, parallel to $Oxyz$, with its origin at the centre of mass of the H_2 molecule (see Fig. 1). In order to define the new coordinate system for ND_2H , we must first anchor the new centre of mass in the old coordinate system, then perform the relevant rotation of the Oxz axes around the invariant Oy axis, which remains perpendicular to the plane of symmetry of the ND_2H molecule. If $O'x'y'z'$ is the new spherical frame centered on the O' centre of mass on ND_2H , and γ the rotation of the $O'z'$ axis around the $O'y'$ axis ($O'y'$ is parallel to Oy), we have according to Cohen & Pickett (1982) :

$$\begin{aligned} x_{O'} &= -0.095957 \text{ Bohr} \\ z_{O'} &= -0.062152 \text{ Bohr} \\ \gamma &= 11.30 \text{ degrees} \end{aligned} \quad (1)$$

It is enough to translate the centre of mass and perform the relevant rotation γ around Oy and O_Hy_H to get the new coordinate system in which the $\text{ND}_2\text{H-H}_2$ PES should be expressed (see Fig. 1). The change of coordinates is given by:

$$\begin{cases} x = x' \cos \gamma - z' \sin \gamma + x_{O'} \\ y = y' \\ z = x' \sin \gamma + z' \cos \gamma + z_{O'} \end{cases} \quad (2)$$

The H_2 internal coordinates are transformed in a similar way, so

that $O'x'y'z'$ and $O_Hx_Hy_Hz_H$ remain parallel and O_H is now located with respect to $O'x'y'z'$ at a distance R' . This corresponds to a pure rotation of γ along the y_H axis:

$$\begin{cases} x_H = x'_H \cos \gamma - z'_H \sin \gamma \\ y_H = y'_H \\ z_H = x'_H \sin \gamma + z'_H \cos \gamma \end{cases} \quad (3)$$

Eventually, the functional form we take is identical to the one for water-hydrogen (Phillips et al. 1994; Valiron et al. 2008). The spherical angles, all primed, refer to the new frames $O'x'y'z'$ and $O_Hx_Hy_Hz_H$:

$$V(R', \theta', \phi', \theta'_H, \phi'_H) = \sum v_{l_1 l_2 l m}(R') t_{l_1 l_2 l m}(\theta', \phi', \theta'_H, \phi'_H), \quad (4)$$

where the function $t_{l_1 l_2 l m}$ are explicitly given in Phillips et al. (1994); Valiron et al. (2008). As previously (Valiron et al. 2008; Maret et al. 2009), we selected iteratively all statistically significant terms $v_{l_1 l_2 l m}(R')$ using the procedure described in Valiron et al. (2008). The final expansion includes anisotropies up to $l_1=10$ for ND_2H and $l_2=4$ for H_2 , resulting in 197 $t_{l_1 l_2 l m}$ functions.

3 COLLISIONAL TREATMENT

In the low temperature environments where ND_2H has been detected the kinetic temperature is below 20 K (Roueff et al. 2000) and the main constituent, H_2 , is expected to lie in its ground rotational (para) state, $J = 0$ (Troscompt et al. 2009). The calculations presented below were restricted to collisions between ND_2H and para- $\text{H}_2(J = 0)$, i.e. by neglecting the $J = 2$ (closed) channel. This latter was actually found to change the cross-sections, at very low energies, by up to a factor of 3, as observed for $\text{NH}_3\text{-H}_2$ (see references in Maret et al. (2009)). Its effect on the average cross-sections and rate coefficients is however much smaller, typically 30 %, which is therefore the typical accuracy of the rates below. The rotational constants of ND_2H were taken from Coudert et al. (1986). The resulting rotational energy levels are given Table 1. The reduced collisional mass is $\mu = 1.822684$ amu.

Full quantum close coupling (CC) scattering calculations were performed with help of the Molscat program (Hutson & Green 1995) which computes scattering matrices (S matrices) and combines these in order to determine elastic and inelastic cross sections, at defined total energies E . The convergence of the inelastic cross sections was checked to be better than 5%, for the different rotational transitions investigated here. The different collision parameters defined in Molscat are given the default ones. We used the following values : $\text{RMIN} = 3.0$, $\text{INTFLG} = 6$, $\text{STEPS} = 10.0 - 30.0$. Calculations have been performed for total energies between 10 cm^{-1} and 430 cm^{-1} . The energy step has been varied with increasing collision energy. It was 0.25 cm^{-1} for a total energy between 10 cm^{-1} and 40 cm^{-1} , 1 cm^{-1} between 40 cm^{-1} and 80 cm^{-1} , 5 cm^{-1} between 80 cm^{-1} and 100 cm^{-1} and 20 cm^{-1} above 100 cm^{-1} . The size of the rotational basis set of ND_2H was also varied with energy. For $E \leq 100 \text{ cm}^{-1}$, $J(\text{ND}_2\text{H}) \leq 10$; at $E = 120 \text{ cm}^{-1}$, $J(\text{ND}_2\text{H}) \leq 12$. For the CS calculations at $E \geq 150 \text{ cm}^{-1}$, $J(\text{ND}_2\text{H}) \leq 16$.

In order to limit the time of computation needed for a scattering calculation, some customary approximations of the collisional treatment are implemented in the Molscat program such as the Coupled State (CS) approximation introduced by McGuire & Kouri (1974). In this approximation, scattering equations are written in the body-fixed frame which is rotating. Then the projection of the

Table 1. Rotational level energies for ND₂H, as used in our computation.

$J_{K_a K_c}$	Energy (cm ⁻¹)
0 ₀₀	0
1 ₀₁	9.09393
1 ₁₁	11.19743
1 ₁₀	12.78456
2 ₀₂	26.65954
2 ₁₂	27.79543
2 ₁₁	32.55350
2 ₂₁	38.86400
2 ₂₀	39.48154

orbital angular momentum l is restricted to the value $m_l = 0$. The accuracy of this method is questionable but it was shown to agree with CC calculations within typically $\sim 30\%$ for the present system, as shown below. Here we resorted to the CS approximation for total energies $E \geq 150$ cm⁻¹. As a result, at the low temperatures at which the rates were calculated ($T \leq 35$ K), the sensitivity to the CS calculations was checked to be marginal.

4 RESULTS

Figure 2 displays the collisional de-excitation cross sections corresponding to the transition $1_{11} \rightarrow 0_{00}$ and $1_{10} \rightarrow 1_{01}$ as a function of the relative kinetic energy between ND₂H and H₂, both at the CC and CS level. These transitions are observable from the ground at 335 and 110 GHz and are potentially important probes of cold prestellar cores (Lis et al. 2006; Gerin et al. 2006; Roueff et al. 2000). For comparison, also cross sections with He computed at the CS level, from Machin & Roueff (2007), are shown. A complex resonance structure is seen for energies smaller than about 100 cm⁻¹ with broad and narrow features, resulting in large variations of the cross sections. The sharp maxima are due to the opening of new collision channels and correspond to both Feshbach and shape resonances. This is in contrast with the He-NHD₂ collision case, with a much shallower potential well. Even if the symmetry of the two problems are identical, differences arise in their cross-section structures and cross section values. A similar effect was found recently at much higher energies, for the differential inelastic cross section of water-H₂, $J = 0$ compared with water-He (Yang 2010). As is always been observed, the resonances quickly disappear with increasing energy. The cross sections relative to Helium are significantly smaller in the energy range displayed in Figure 2. However, they converge to those involving para-H₂ at collision energies above ~ 80 cm⁻¹.

Knowing the importance of the hyperfine quadrupolar effect for ¹⁴N, nuclear spin $I = 1$, extending those cross section calculations to include explicitly the hyperfine structure could be of interest. Hyperfine structure has indeed been observed with some precision in the lower transitions (Gerin et al. 2006). However, because of the low symmetry of NHD₂ (asymmetric top), no close formula exist in the literature that could connect state to state hyperfine rates to state to state global rotational rates. One should resort to a full summation of S matrix elements in order to get all detailed hyperfine rates. Also, because of the small column density of NHD₂, the differential effects on the various hyperfine lines should remain small (Daniel et al. 2006).

The collisional (de)excitation rates R as a function of temperature T were obtained by a Maxwell-Boltzmann averaging of the cross sections times the relative velocity. In the equation below, E_{kin} is the relative kinetic energy:

$$R_{J_{K_a K_c} \rightarrow J'_{K'_a K'_c}}(T) = \left(\frac{8k_B T}{\pi \mu} \right)^{\frac{1}{2}} \left(\frac{1}{k_B T} \right)^2 \int_0^{\infty} \sigma_{J_{K_a K_c} \rightarrow J'_{K'_a K'_c}}(E_{kin}) \exp\left(-\frac{E_{kin}}{k_B T}\right) E_{kin} dE_{kin} \quad (5)$$

k_B is the Boltzmann constant and μ is the reduced mass of the ND₂H - H₂ system. Cross sections having been computed for collision energies up to above 390 cm⁻¹, the rate coefficients may be calculated very safely for temperatures between 5 K and 35 K which are relevant for cold prestellar cores. Table 2 gives the de-excitation rate coefficients for the 9 first rotational levels as well as the fitting parameters allowing to display the rate coefficients for any temperature between 5 and 35 K *via* the following expression (Faure, Gorfinkiel, & Tennyson 2004), with R in 10⁻¹¹ cm³.s⁻¹:

$$\log_{10} R(T) = \sum_0^3 a_n T^{-n/6} \quad (6)$$

All fits have been verified to be precise to better than 1 %. It should be noted that the following inelastic transitions are strictly forbidden in the CS approximation (owing to spurious selection rules): $1_{01} \rightarrow 0_{00}$, $2_{12} \rightarrow 0_{00}$ and $2_{11} \rightarrow 0_{00}$. We see that the corresponding CC rates are not negligible, although about one order of magnitude smaller than the largest rates. There is therefore no obvious collisional propensity rules for the presented transitions. We note that since the dipole moment has two non-zero projections (μ_b and μ_c), the corresponding radiative selection rules are $\Delta J = 0, 1$ and $\Delta K_a = \pm 1$, $\Delta K_c = \pm 1$ for transitions along μ_b and $\Delta K_a = \pm 1$, $\Delta K_c = 0, \pm 2$ for transitions along μ_c . The Einstein coefficients have been computed by Coudert and Roueff (2006) and recalled in Machin & Roueff (2007).

5 DISCUSSION AND CONCLUSIONS

The comparison of the present rates with the values obtained by Machin & Roueff (2007) where Helium is the collider is informative. The collision rates obtained in the present work when para-H₂ ($J=0$) is the perturber are typically one order of magnitude larger than those obtained with Helium. The origin of this discrepancy lies in the significantly different potential wells of the NH₃-H₂ and NH₃-He PES, as discussed by Maret et al. (2009). The usual scaling between the collision rates obtained from the ratio of the reduced masses is clearly not accurate and the calculations have to be performed explicitly in order to obtain the appropriate rates with molecular hydrogen. We display in Table 3 the resulting critical densities for the para and ortho transitions. These were obtained by simply dividing the Einstein coefficient of a given transition by the corresponding de-excitation rate coefficient at 10 K. Note that other definitions are possible (Maret et al. 2009). These values set the limit of the perturber density above which the transitions become thermalized. We see that the critical densities corresponding to the two transitions $1_{11} \rightarrow 0_{00}$ and $1_{10} \rightarrow 0_{00}$ are different by about one order of magnitude at 10 K, which is about a factor of 3 less than the ratio of the Einstein coefficients. Such differences may have profound consequences on the interpretation of these two transitions which are both observable from the ground (Lis et al. 2006; Gerin et al. 2006) at 335 and 389 GHz respectively, as the

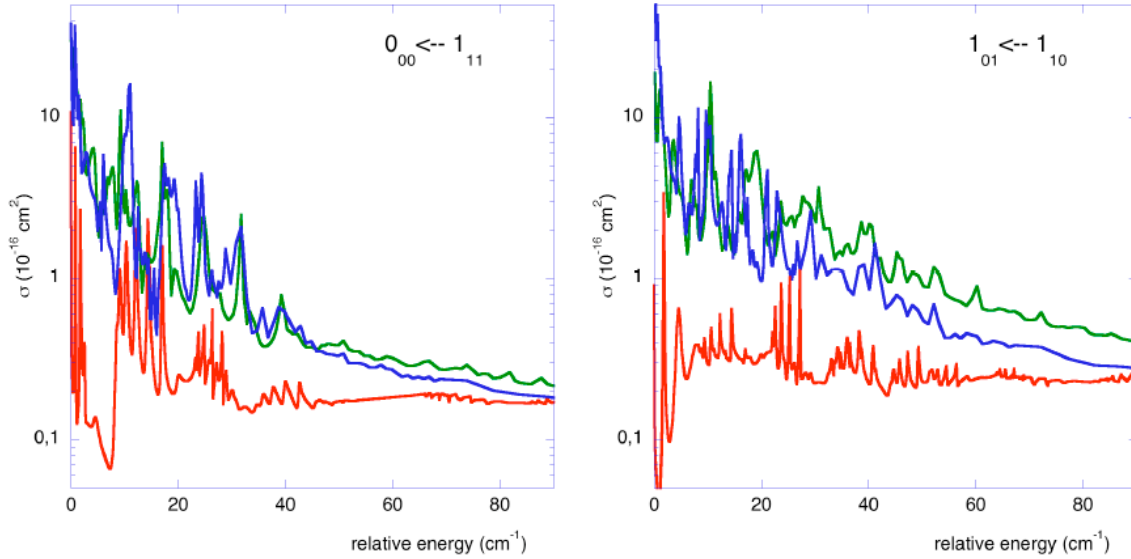


Figure 2. Collisional de-excitation cross sections as a function of the relative kinetic energy. Left: transition $1_{11} \rightarrow 0_{00}$ of ND_2H with Helium in CS approximation (red) ((Machin & Roueff 2007)) and para H_2 (present work) in CC (blue) and CS (green) approximations. Right : transition $1_{10} \rightarrow 1_{01}$ of ND_2H with Helium in CS approximation (red)((Machin & Roueff 2007)) and para H_2 (present work) in CC (blue) and CS (green) approximations

Table 3. Calculated critical densities for the first *ortho* and *para* transitions of ND_2H with H_2 at 10 K.

Transition	Critical density (cm^{-3})	
	<i>ortho</i>	<i>para</i>
$1_{11} \rightarrow 0_{00}$	$1.17 \cdot 10^6$	$1.34 \cdot 10^6$
$1_{11} \rightarrow 1_{01}$	$3.48 \cdot 10^4$	$6.63 \cdot 10^4$
$1_{10} \rightarrow 0_{00}$	$1.10 \cdot 10^7$	$1.01 \cdot 10^7$
$1_{10} \rightarrow 1_{01}$	$5.19 \cdot 10^4$	$5.94 \cdot 10^4$
$2_{02} \rightarrow 1_{11}$	$6.34 \cdot 10^5$	$6.76 \cdot 10^5$
$2_{02} \rightarrow 1_{10}$	$5.33 \cdot 10^6$	$5.66 \cdot 10^6$
$2_{12} \rightarrow 2_{02}$	$2.31 \cdot 10^4$	$9.26 \cdot 10^3$
$2_{11} \rightarrow 1_{01}$	$1.14 \cdot 10^8$	$1.18 \cdot 10^8$
$2_{11} \rightarrow 1_{10}$	$1.33 \cdot 10^7$	$1.45 \cdot 10^7$
$2_{11} \rightarrow 2_{02}$	$7.59 \cdot 10^4$	$7.12 \cdot 10^4$
$2_{21} \rightarrow 1_{11}$	$1.80 \cdot 10^8$	$1.79 \cdot 10^8$
$2_{21} \rightarrow 1_{10}$	$4.17 \cdot 10^7$	$1.77 \cdot 10^7$
$2_{21} \rightarrow 2_{12}$	$2.70 \cdot 10^5$	$1.94 \cdot 10^5$
$2_{21} \rightarrow 2_{11}$	$1.39 \cdot 10^6$	$1.23 \cdot 10^6$
$2_{20} \rightarrow 1_{11}$	$5.78 \cdot 10^7$	$2.26 \cdot 10^7$
$2_{20} \rightarrow 1_{10}$	$1.47 \cdot 10^8$	$1.49 \cdot 10^8$
$2_{20} \rightarrow 2_{12}$	$5.65 \cdot 10^6$	$6.44 \cdot 10^6$
$2_{20} \rightarrow 2_{11}$	$3.96 \cdot 10^5$	$2.48 \cdot 10^5$

corresponding upper levels may not be accounted for by a single excitation temperature.

ACKNOWLEDGEMENTS

We are deeply indebted to Pierre Valiron, who gave impetus and ideas throughout the inception of this work. ES was supported by a grant of the "Molecular Universe" FP6 Marie Curie network. We acknowledge support from the French Institut National des Sciences de l'Univers, through its program "Physique et Chimie

du Milieu Interstellaire". LAOG is a joint laboratory Université Joseph-Fourier/CNRS under the name UMR 5571.

REFERENCES

- Benedict W. S., Gailar N. & Plyler E. K., 1957, *Can. J. Phys.*, 35, 1235
- Cohen A. E. & Pickett H. M., 1982, *J. Mol. Spectrosc.*, 93, 83
- Coudert L., Valentin A., & Henry L., 1986, *J. Mol. Spectrosc.*, 120, 185
- Coudert L., Roueff, E., 2006, *Astron. & Astrophys.*, 449, 855
- Daniel F., Cernicharo J., Dubernet M.L. 2006, *ApJ*, 648, 461
- Dubernet M.L. et al., 2006, *A&A*, 460, 323
- Garrison B. J., Lester W. A., Miller W. H., 1976, *J. Chem. Phys.*, 65, 2193
- Faure A., Gorfinkiel J. D., Tennyson J., 2004, *MNRAS*, 347, 323
- Faure A., Valiron P., Wernli M., Wiesenfeld L., Rist C., Noga J., Tennyson J., 2005, *J. Chem. Phys.*, 122, 1102
- Garrison B. J. & Lester W. A., 1977 *J.Chem.Phys.*, 66, 531
- Gerin, M., Lis, D. C., Philipp, S., Guesten, R., Roueff, E., and Reveret, V., 2006, *A&A*, 454, L63
- Phillips, T.R., Maluendes, S., McLean, A. D. and Green, S., 1994, *J. Chem. Phys.*, 101, 5824
- Hodges M. P. and Wheatley R. J., 2001, *J.Chem.Phys.*, 114, 8836
- Larsson B., Liseau R., Bergman P. et al., 2003, *A&A*, 402, L69
- Lis, D. C., Gerin, M., Roueff, E., Vastel, C., Phillips, T.G., 2006, *ApJ*, 636, 916
- Loinard, L., Castets, A., Ceccarelli, C., Caux, E., Tielens, A.G.G.M., 2001, *ApJ*, 552, L163
- Machin L., Roueff E., 2005, *J. Phys. B: At. Mol. Opt. Phys.*, 38, 1519
- Machin L., Roueff E., 2006, *A&A*, 460, 953
- Machin L., Roueff E., 2007, *A&A*, 465, 647
- Maret S., Faure A., Scifoni E., Wiesenfeld L., 2009, *Mon. Not. R. Astr. Soc.*, 399, 425

Table 2. Deexcitation rate coefficients for ND₂H-para H₂ ($J = 0$) collisions. Fits to formula (6) are given in the last 4 columns.

Temperature	Rate coefficients R_{if} (10^{-11} cm ³ .s ⁻¹)							Fit coefficients				
	5K	10K	15K	20K	25K	30K	35K	a_n	0	1	2	3
1 ₀₁ → 0 ₀₀	0.572	0.436	0.351	0.29	0.245	0.211	0.183		19.71	-46.57	37.81	-10.74
1 ₁₁ → 0 ₀₀	1.14	1.10	1.03	0.938	0.854	0.781	0.717		22.53	-51.13	38.73	-9.74
1 ₁₁ → 1 ₀₁	7.57	6.79	6.14	5.62	5.21	4.89	4.63		0.00	-3.51	5.63	-1.38
1 ₁₀ → 0 ₀₀	4.75	4.39	4.05	3.74	3.49	3.29	3.13		1.89	-7.36	8.07	-2.04
1 ₁₀ → 1 ₀₁	1.49	1.34	1.23	1.12	1.03	0.953	0.887		15.74	-35.56	27.24	-6.91
1 ₁₀ → 1 ₁₁	1.37	1.25	1.14	1.05	0.959	0.887	0.826		14.76	-33.90	26.31	-6.76
2 ₀₂ → 0 ₀₀	0.824	0.782	0.71	0.64	0.581	0.532	0.493		6.58	-19.33	17.89	-5.40
2 ₀₂ → 1 ₀₁	1.13	0.842	0.709	0.613	0.537	0.476	0.425		30.13	-63.93	46.67	-11.72
2 ₀₂ → 1 ₁₁	3.19	3.06	2.97	2.90	2.83	2.77	2.73		2.52	-5.88	4.76	-0.82
2 ₀₂ → 1 ₁₀	1.29	1.12	1.00	0.904	0.821	0.752	0.694		15.98	-36.13	27.88	-7.23
2 ₁₂ → 0 ₀₀	0.275	0.272	0.234	0.199	0.171	0.148	0.13		6.25	-24.01	24.97	-8.41
2 ₁₂ → 1 ₀₁	3.95	3.84	3.73	3.61	3.52	3.44	3.37		1.09	-3.63	3.67	-0.58
2 ₁₂ → 1 ₁₁	0.808	0.868	0.823	0.753	0.684	0.623	0.569		15.88	-40.31	32.97	-8.84
2 ₁₂ → 1 ₁₀	0.739	0.787	0.744	0.683	0.621	0.565	0.516		17.41	-43.09	34.66	-9.22
2 ₁₂ → 2 ₀₂	3.40	3.77	3.97	4.03	4.03	4.01	3.99		11.93	-25.60	17.74	-3.40
2 ₁₁ → 0 ₀₀	0.104	0.116	0.102	0.0875	0.0749	0.0647	0.0564		2.64	-19.41	23.36	-8.68
2 ₁₁ → 1 ₀₁	1.95	2.22	2.36	2.40	2.40	2.38	2.35		16.14	-34.63	24.05	-5.07
2 ₁₁ → 1 ₁₁	3.72	4.02	4.14	4.14	4.08	3.98	3.88		18.59	-39.65	27.74	-5.77
2 ₁₁ → 1 ₁₀	0.464	0.489	0.464	0.428	0.393	0.362	0.336		10.75	-28.86	24.57	-7.06
2 ₁₁ → 2 ₀₂	2.78	2.99	3.00	2.96	2.90	2.85	2.81		-1.02	-0.82	2.40	-0.45
2 ₁₁ → 2 ₁₂	1.08	1.25	1.23	1.15	1.07	1.00	0.943		2.38	-13.06	14.38	-4.38
2 ₂₁ → 0 ₀₀	0.341	0.346	0.342	0.334	0.325	0.317	0.311		4.09	-10.33	8.44	-2.71
2 ₂₁ → 1 ₀₁	3.41	3.86	3.98	3.93	3.82	3.69	3.57		15.47	-35.32	26.13	-5.71
2 ₂₁ → 1 ₁₁	2.21	2.33	2.43	2.48	2.50	2.50	2.50		13.36	-26.93	17.69	-3.41
2 ₂₁ → 1 ₁₀	0.616	0.593	0.577	0.554	0.529	0.506	0.486		17.15	-36.63	26.22	-6.52
2 ₂₁ → 2 ₀₂	1.55	1.34	1.20	1.10	1.01	0.947	0.896		3.52	-9.97	9.64	-2.92
2 ₂₁ → 2 ₁₂	3.50	3.02	2.75	2.56	2.41	2.29	2.19		4.43	-10.36	8.80	-2.11
2 ₂₁ → 2 ₁₁	1.93	2.07	2.10	2.09	2.05	2.00	1.96		10.90	-24.41	17.82	-3.94
2 ₂₀ → 0 ₀₀	2.43	2.39	2.31	2.20	2.11	2.02	1.95		6.54	-16.01	12.96	-3.09
2 ₂₀ → 1 ₀₁	0.631	0.649	0.649	0.638	0.625	0.612	0.600		6.85	-15.70	11.80	-3.10
2 ₂₀ → 1 ₁₁	0.441	0.408	0.389	0.367	0.346	0.327	0.309		21.50	-45.57	32.53	-8.20
2 ₂₀ → 1 ₁₀	2.98	3.00	3.03	3.04	3.03	3.02	3.00		7.58	-15.32	10.22	-1.77
2 ₂₀ → 2 ₀₂	1.86	1.66	1.56	1.47	1.40	1.33	1.27		14.77	-31.02	22.26	-5.22
2 ₂₀ → 2 ₁₂	1.09	1.02	0.998	0.97	0.938	0.906	0.876		20.42	-41.66	28.53	-6.55
2 ₂₀ → 2 ₁₁	0.897	0.992	1.03	1.03	1.02	1.00	0.989		10.70	-24.06	17.45	-4.11
2 ₂₀ → 2 ₂₁	0.405	0.379	0.365	0.346	0.324	0.303	0.284		32.14	-67.28	47.18	-11.49

Meuwly, M and Bemish R.J., 1997, J.Chem.Phys., 106, 8672

McGuire P., Kouri D. J., 1974, J.Chem.Phys., 60, 2488

Hutson J. M. & Green S., 1995, Molscat computer code, version 14, distributed by collaborative computational project 6 of the Science and Engineering Research Council (UK)

Müller H. S. P., Thorwirth S., Roth D. A. & Winnewisser G., 2001, A&A, 370, L49

Palma A. & Green S., 1987, ApJ, 316, 83

Räjamäki T., Kállay M., Noga J., Valiron P., Halonen L., 2004, Mol. Phys., 102, 2297

Roueff E., Tiné S., Coudert, L.H., Pineau des Forêts G., Falgarone E., Gerin M., 2000, A&A, 354, 63

Roueff E., Lis, D.C., van der Tak F.F.S., Gerin M., Golsmith, P.F., 2005, A&A, 438, 585

Scifoni E., Valiron P., Faure A., Rist C., 2007, in Molecules in

Space and Laboratory, J.L Lemaire & F. Combes (eds.), p130

Scribano Y., Faure A. and Wiesenfeld L., 2010 J.Chem.Phys., in print.

Townes C. H. & Schawlow A. L., 1975, Microwave Spectroscopy, ed. Dover Publications, New York

Troscompt N., Faure A., Maret S., Ceccarelli C., Hily-Blant P., Wiesenfeld L., 2009, A&A, 506, 1243

Valiron P., Wernli M., Faure A., Wiesenfeld L., Rist C., Kedžuch S. and Noga J., 2008, J.Chem.Phys., 129, 134306

Wolniewicz L., 1995, J.Chem.Phys.103, 1792

Yang C.-H., Sarma G., Ter Meulen J. J., Parker D. H., McBane G. C., Wiesenfeld L., Faure A., Scribano Y., and Feautrier N., 2010, J. Chem. Phys., 133, 131103